Origin of Anomalous Pt–Pt Distances in the Pt/Alumina Catalytic System

Karl Sohlberg,*[a] Sergey Rashkeev,[b] Albina Y. Borisevich,[c] Stephen J. Pennycook,[b, c] and Sokrates T. Pantelides[b, c]

The Pt/γ-alumina system is representative of many common heterogeneous catalysts, which consist of transition metals dispersed on a high surface-area support. For example, catalytic reduction and oxidation of automotive pollutants is accomplished with platinum (Pt) or rhodium (Rh) dispersed on a γ-alumina surface.[1] Olefin cracking is carried out on catalysts formed by dispersal of transition-metal atoms on insulating supports,[2] such as zeolites[3] or alumina.[4] The Cr/alumina system is used for dehydrogenation of alkanes to form starting materials for chemical synthesis.[5] Prerequisite to the nonempirical design and refinement of improved catalysts is the identification of the atomic-scale structure and properties of the catalytically active sites. This has become a major industrial research priority.

It has long been recognized that electron microscopy is a powerful tool for investigating supported catalysts.[6,7] *Z*-contrast imaging in scanning transmission electron microscopy (*Z*-STEM, where *Z* denotes nuclear charge) is capable of imaging individual atoms on real (i.e., not idealized) catalytic supports.[8] Application of *Z*-STEM to the Pt/γ-alumina catalytic system suggested the presence of intriguing atomic-scale structures.[8] In addition to isolated Pt atoms, trimers of Pt are observed with preferred shapes that are inconsistent with those of gas-phase transition metal clusters[9] and exhibit atypical Pt–Pt distances. Trimers of Pt on γ-alumina have also been inferred from average coordination number as determined by extended X-ray absorption fine structure measurements.[10] These supported clusters are qualitatively different from larger Pt aggregates on γ-alumina revealed by transmission electron microscopy (TEM) studies.[11,12]

First-principles calculations have been used to yield detailed structural information about supported metal clusters.[7,13] For example, theoretical investigations have been reported for small clusters of Pt[9] and Pd[9,14] on α-alumina.

Herein, we report new subangstrom-resolution *Z*-STEM images of the Pt/γ-alumina system that confirm the presence of the perplexing Pt_3 structures. We then apply first-principles density functional theory calculations to test several hypotheses about the structure of these supported clusters. These studies reveal three key features of the Pt/γ-alumina system: 1) Oxygen termination of the alumina surface is favored; 2) Adatom Pt structures are thermodynamically preferred over substitutional Pt structures; 3) Pt_3 structures with anomalously long Pt–Pt distances are stabilized by –OH caps.

[a] Prof. K. Sohlberg
Department of Chemistry, Drexel University
3141 Chestnut Street, Philadelphia, PA 19104 (USA)
Fax: (+1) 215-895-1265
E-mail: sohlbergk@drexel.edu

[b] Prof. S. Rashkeev, Prof. S. J. Pennycook, Prof. S. T. Pantelides
Department of Physics and Astronomy, Vanderbilt University
Nashville, TN 37235 (USA)

[c] Dr. A. Y. Borisevich, Prof. S. J. Pennycook, Prof. S. T. Pantelides
Condensed Matter Sciences Division, P.O. Box 2008
Oak Ridge National Laboratory, Oak Ridge, TN 37831-6031 (USA)

Experimental Section

Microscopy: *Z*-contrast STEM images were obtained with a VG Microscopes HB603U operating at 300-kV electron energy and equipped with a Nion™ aberration corrector to give a probe size of 0.7–0.8 Å.[15] The *Z*-contrast mode uses an annular detector to detect electrons scattered to high angles. Rutherford scattering from the atomic nuclei predominates, with a cross-section proportional to Z^2. A high-*Z* catalyst atom on a low-*Z* support therefore gives a spot with high contrast and with a size equal to the microscope probe size.

Theory: The calculations were carried out with density functional theory[16] and the generalized gradient approximation (GGA) was employed to obtain the exchange-correlation energy (V_{XC}),[17,18] as described by Payne et at. and coded in the Cambridge serial total energy package (CASTEP).[19] Electron–ion interactions were described with the ultrasoft reciprocal-space pseudopotentials of Vanderbilt et al.[20] A plane wave basis with a cutoff energy of 380 eV was used to describe the electronic density. Integrations over the Brillouin zone employed a grid of *k* points with a spacing of 0.1 $Å^{-1}$ chosen following the Monkhorst–Pack scheme.[21] (4 *k* points for bulk calculations, 3 *k* points for surface cells) The local charge distribution was investigated with charge density plots and by Mulliken population analysis as implemented by Segall.[22]

Bulk structural relaxation, including unit cell optimization, was carried out for γ-alumina in its fully hydrogenated form[23] based on the HAl_5O_8 primitive cell (space group Fd3m). The computed cell parameters (in Å and degrees) are: $a=5.443$, $b=5.503$, $c=5.503$, $\alpha=60.6$, $\beta=60.5$, $\gamma=60.5$. The computed material density (3.72 g mL^{-1}) varies minimally from the experimental value (3.5 g mL^{-1})[24] and form that obtained by all-electron calculations (3.53 g mL^{-1}).[25] The surface structural relaxation studies employed infinitely repeating slabs of γ-alumina 5 layers thick with a vacuum spacing between the slabs of 10 Å. The top layer was the preferentially exposed (110C) layer.[26] The atoms in the bottom layer were frozen, as were the dimensions (a, b, c, α, β, γ) of the unit cell. Previous studies of the γ-alumina demonstrated that at 5 layers surface structure is converged with respect to increasing the slab thickness.[27,28] Optimizations were taken to be converged when the change between iterations was less than the following values: total energy 2.0×10^{-5} eV per atom, root mean square (RMS) displacement of atoms 1.0×10^{-3} Å, RMS force on atoms 5.0×10^{-2} eV $Å^{-1}$, and (for unit cell optimizations) the RMS of the stress tensor 1.0×10^{-1} GPa. As reviewed in ref. [29], these surface models are consistent with neutron scattering, X-ray scattering data, atomic-resolution electron microscopy and high-resolution surface IR data. They have been been found critical to explain subtle surface chemistry effects.[13,30]

 DOI: 10.1002/cphc.200400212 © 2004 Wiley-VCH Verlag GmbH & Co. KGaA, Weinheim

Results and Discussion

A representative atomic resolution *Z*-STEM image of a bimetallic Pt-Ru/γ-alumina catalyst prepared as described in ref. [31] is shown in Figure 1. The resolution exceeds, by a factor of two or more, all previously published *Z*-STEM images of Pt on γ-alumina.[8] Consequently, the heavy Pt atoms give rise to bright, well-resolved spots, and fringes from scattering by the light support are also visible. From the complementary phase-contrast image, the support material is found to be near the (110) orientation.[8] Examples of Pt trimers are circled.

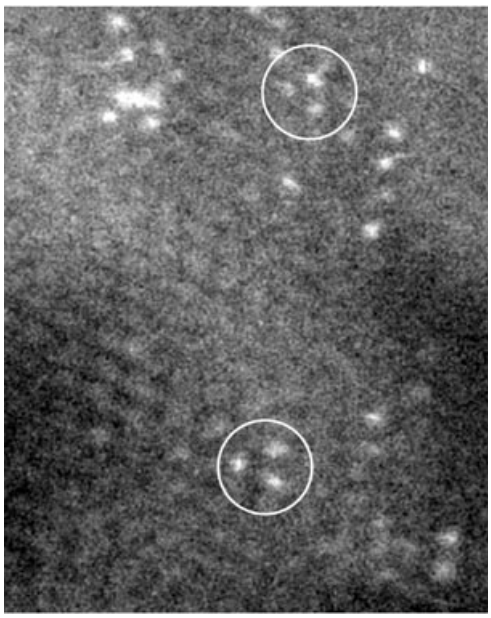

Figure 1. *Z-contrast STEM image of Pt on the (110) surface of γ-alumina. Two Pt_3 (trimer) structures are circled. A hint of the alumina lattice is also visible.*

Figure 2 depicts an edge-on view of the top 5 layers of γ-alumina exposing the preferred (110C) face.[28] Previous calculations have shown that there is an energetic preference for the hydrogen atoms to occupy nominal tetrahedral sites within the spinel lattice.[23] Rather than residing at the perfect T_d cation site, however, each H atom forms an OH group with one of the four nearest neighbor oxygen atoms. This symmetry breaking is of little consequence in bulk γ-alumina,[32] but at the surface, it gives rise to several distinguishable distributions of the H atoms. At the (110C) surface, H atoms will nominally appear in the "trenches" that naturally appear on the surface, and in tetrahedral sites in the second subsurface layer. We denote the four unique positions A0, A1, B0 and B1 in Figure 2. Here A or B denote the position within the nominal T_d site, and 0 or 1 denote the surface or third layer, respectively. Full structural relaxations for the (A0 & A1), (A0 & B1), (B0 & A1) and (B0 & B1) H distributions show that the position of the H atom within the site in the third layer is of little significance, with less than 0.01 eV difference between the A and B positions, (not meaningful given the accuracy of the present calculations) but on the surface, the A position is energetically preferred by about 0.1 eV. The energetically preferred (A0A1) distribution of H atoms was selected as the starting point in all subsequent calculations.

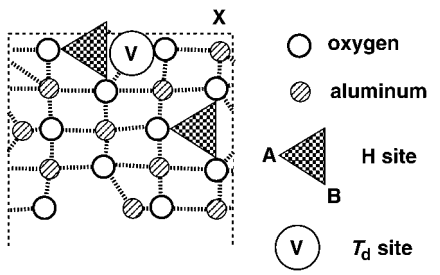

Figure 2. *Edge-on view of the top five atomic layers of γ-alumina exposing the (110C) face. This is an edge-on view of the full structure shown in Figure 4. The site marked by a circled "V" is nominally a T_d cation site, but is vacant in the fully optimized surface.[28] Nominal T_d hydrogen sites are indicated by the checkerboard triangles. A hydrogen atom in such a site associates more closely with one of the four oxygen atoms at the vertices of the tetrahedron. "A" or "B" denotes this position within the nominal T_d site. The "0" or "1" subdesignation used in the text denotes whether the site is in the surface layer or third layer, respectively. (There are two "A" positions in each nominal T_d hydrogen site, one behind the other in this view. These are denoted "A" and "A′" in Figure 3.) X marks the position of oxygen adatoms when the surface is oxygen-terminated.*

First, we considered isolated Pt adatoms. As throughout this work, we reference the energies to an undoped surface slab plus three atoms of bulk Pt metal. The actual formation of Pt/γ-alumina uses complex multi-element reagents,[31] but since we are dealing with state functions, the above serves as a convenient common reference from which to determine relative energies. Four chemically reasonable trial structures were identified for a Pt adatom on the γ-alumina surface: 1) Pt atom near the center of the surface "trench" (+2.3 eV); 2) Pt atom above a surface O atom (+1.8 eV); 3) Pt atom above a surface Al atom (+2.2 eV); 4) Pt atom above a surface OH group (+4.6 eV). Here the relative energy is given in parenthesis. Structure 2 is the lowest energy configuration for a single Pt adatom (see Figure 3).

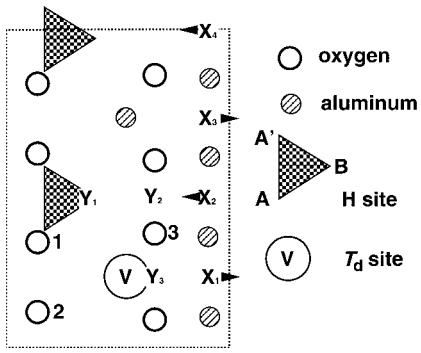

Figure 3. *Schematic top view of the γ-alumina (110C) face. This is a top-down view of the full structure shown in Figure 4. A substitutional Pt_3 (trimer) may be formed by replacing oxygen #1, oxygen #2, and the aluminum vacancy by Pt. A substitutional Pt_2 (dimer) may be formed by replacing either oxygen #1 or oxygen #2 and the aluminum vacancy by Pt. The energetically favored position for a Pt adatom is above oxygen #3, bridging to the adjacent Al to its right. X_i mark the positions of oxygen adatoms when the surface is oxygen terminated. When oxygen terminated, a metastable Pt_3OH structure is formed by placing Pt atoms at the positions Y_i (i = 1.3). This structure is consistent in geometry with the Z-STEM image. See caption of Figure 2 for other legend details.*

 © 2004 Wiley-VCH Verlag GmbH & Co. KGaA, Weinheim

Next, we considered clusters of two or three Pt adatoms. The lowest energy adatom dimer (trimer) was found to have an energy of +3.8 eV (+8.5 eV). This shows that the energy of formation for a cluster of *n* Pt atoms on the Al–O-terminated slab is greater than the formation energy for placing *n* isolated Pt atoms on the surface. Supported cluster formation by coalescence of isolated Pt adatoms is apparently energetically unfavorable. This chemistry is similar to that of Pt on MgO[33] but very different from that of the Rh/γ-alumina system, where Rh is seen to agglomerate into raftlike structures.[8] The observed Pt clusters are evidently not simple adatom structures.

γ-Alumina is an intrinsically highly defective structure with an unusual surface chemistry that facilitates the creation of Al and O vacancies in the surface.[34] We have therefore investigated the possibility that the observed Pt structures form at surface defects. One obvious possibility is that a Pt atom may fill a T_d cation site in the surface layer. Previous studies have demonstrated that vacancies at such sites are formed by a barrierless reconstruction of the γ-alumina (110C) surface.[34] Another possibility is that Pt atoms fill oxygen vacancies created by the "reactive sponge" surface chemistry of γ-alumina.[23] Simultaneous substitution of Pt into two or three adjacent sites could result in the formation of dimers or trimers. We tested four possibilities: 1) Pt occupying a T_d cation site in the surface. 2) Pt occupying an oxygen site in the surface; 3) Two Pt atoms, one occupying a T_d cation site in the surface and the other an adjacent oxygen site to form a dimer; 4) Three Pt atoms, one occupying a T_d cation site in the surface and the other two filling adjacent oxygen sites to form a trimer. These structures are depicted schematically in Figure 3, which is a top-down view of the full structure shown in Figure 4. The insertion of Pt into the γ-alumina surface is accompanied by the loss of H_2O, H_2 and/or O_2 from the surface. We combined the computed total energy data with tabulated third-law entropies to estimate the entropic contributions.[35] Table 1 shows that the entropic contribution does not qualitatively change the predictions.

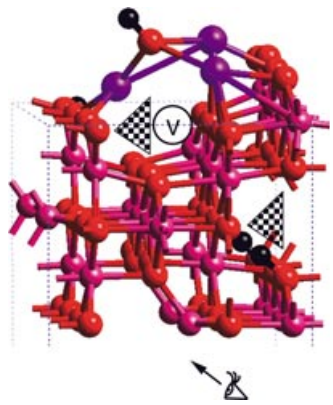

Figure 4. *View of the –OH capped Pt trimer on the oxygen-terminated alumina slab. Figure 2 is a schematic of this structure viewed obliquely from the position of the eye. Figure 3 is a schematic of the top layer of the alumina slab as viewed from above.*

Table 1. *Energies of Pt adatoms and Pt substitutionals on γ-alumina (110C) relative to a bare undoped slab and bulk Pt metal. $Pt_{4(s)}$ and $Al_{4(s)}$ are unit cells of the respective metals; H_2, O_2, and H_2O are considered to be ideal gases. Energies are given in [eV]. Note that the lowest energy Pt-containing structure is an –OH capped Pt_3 (trimer) on an oxygen-terminated (O-term.) surface (sub. = substituting).*

Description	Stoichiometry	ΔG 0 K	ΔG 1000 K
bare slab (reference)	$H_4Al_{26}O_{40}+(3/4)Pt_{4(s)}$	0.0	0.0
O-terminated slab	$H_4Al_{26}O_{44}+(3/4)Pt_{4(s)}-(2)O_{2(g)}$	−4.9	−0.7
Pt adatom	$H_4Al_{26}O_{40}Pt_1+(1/2)Pt_{4(s)}$	1.8	1.8
Pt sub. O position	$H_3Al_{26}O_{39}Pt_1+(1/2)Pt_{4(s)}+(1/2)H_{2(g)}+(1/2)O_{2(g)}$	7.4	5.7
Pt sub. Al position	$H_3Al_{25}O_{40}Pt_1+(1/2)Pt_{4(s)}+(1/2)H_{2(g)}+(1/4)Al_{4(s)}$	8.7	8.0
substitutional Pt_2	$H_2Al_{25}O_{39}Pt_2+(1/4)Pt_{4(s)}+(1/4)Al_{4(s)}+H_2O_{(g)}$	10.5	8.5
substitutional Pt_3	$H_2Al_{25}O_{38}Pt_3+(1/4)Al_{4(s)}+H_2O_{(g)}+(1/2)O_{2(g)}$	13.7	10.7
Pt_3OH on O-term. slab	$H_4Al_{26}O_{45}Pt_3-(5/2)O_{2(g)}$	−3.8	1.4

The calculations indicate that the Pt_3 structure formed when three Pt atoms fill two O vacancies and one Al vacancy (see Figure 3) is metastable, that is, its energy is high but there is a barrier to its dissociation. The computed Pt–Pt distances are: 2.59, 2.65, and 2.73 Å. These distances are consistent with typical Pt–Pt bond distances,[36,37] but do not agree with the experimental Pt–Pt distances observed here of: 2.7±0.2, 3.2±0.2, and 3.4±0.2 Å or with earlier measurements:[8,38] 2.88±0.3, 3.21±0.3, and 3.49±0.3 Å.

Based on these results, Pt structures stabilized by surface vacancies may be effectively ruled out. First, all substitutional structures are thermodynamically unfavorable. Second, even in the event that pre-existing vacancies render the energy cost moot, the observed trimer structures are geometrically inconsistent with the only substitutional Pt_3 structure found by theoretical calculations.

It has been suggested that alumina surfaces are plausibly anion terminated.[26] Oxygen termination is accomplished by bridging adjacent O_h (four-coordinated) Al atoms on the surface with Al–O–Al structures. Oxygen termination completes the six-fold coordination of the surface Al in O_h sites. The positions of the "extra" oxygen atoms are shown in Figure 3 as X_i ($i=1.4$). Upon full structural relaxation the extra row of oxygen atoms forms a slightly zig-zag arrangement as shown (greatly exaggerated) by the arrows in Figure 3.

Chemically, the oxygen termination process may be written as given in Equation (1)

$$H_4Al_{26}O_{40}(\text{Al–O-terminated}) + 2\,O_2(g) \rightarrow H_4Al_{26}O_{44}(\text{O-terminated}) \quad (1)$$

For this process the change in internal energy is computed to be $\Delta E=-4.5$ eV per unit cell or about −1.12 eV per oxygen

 © 2004 Wiley-VCH Verlag GmbH & Co. KGaA, Weinheim

atom. Clearly, oxygen termination is strongly preferred. We estimate the formation energy for an oxygen vacancy on the oxygen-terminated surface by removing two oxygen atoms from nonadjacent positions (such as X_1 and X_3 in Figure 3) to form O_2. The energy change for this process is $\Delta E = 0.94$ eV per oxygen atom.

Given that Pt adatoms are lower in energy than substitutional Pt atoms, and given that the oxygen terminated surface is energetically favored over the Al–O-terminated surface, we investigated the possibility of the formation of Pt adatom clusters on the oxygen-terminated surface. Only one trimer structure was found. The nominal (initial) Pt positions are shown as Y_i ($i = 1.3$) in Figure 3. After full structural relaxation, the computed Pt–Pt distances were found to be: 2.6, 2.6 and 3.3 Å. These are outside the error bounds of the experimentally observed Pt_3 structures. We found, however, that if the Pt_3 structure is "capped" with an –OH group, the computed distances are 2.6, 3.1 and 3.6 Å, in good agreement with the experimentally observed distances. This is the only Pt-containing surface that is lower in energy than the undoped reference slab. Furthermore, relative to the oxygen-terminated surface slab, the surface displaying an –OH capped Pt_3 structure is just 1.16 eV higher in energy. This is about +0.4 eV per Pt atom, a much lower energy cost than the addition of isolated Pt adatoms. The formation of the entire Pt_3OH structure is comparable in energy cost to the formation of a single O vacancy. This result bears some similarity with the stabilization of Pt dimers on α-alumina by adjacent ad-OH.[33] Alternative capping structures were tried: An –O only cap is energetically unfavorable compared to an –OH cap. Capping with a –CO impurity leads to Pt–Pt distances similar to those of an uncapped Pt trimer, that is, not consistent with experimental observations.

Mulliken population analysis (see Table 2) shows that isolated Pt adatoms and Pt atoms filling oxygen vacancies in the surface are nearly valance-neutral to slightly electron-rich. In contrast, the Pt atoms in the –OH capped Pt trimer on the oxygen-terminated surface bear significant valance unsaturation. While the actual charges determined by population analysis are only qualitatively reliable, taking electron depletion as a signature of Lewis acidity, it is reasonable to conclude that the supported clusters should be better Lewis acid sites than isolated Pt adatoms, that is, the former show greater valance unsaturation.

Table 2. Mulliken charges [esu] for Pt atoms on γ-alumina (110C). Note that the Pt atoms in an –OH capped Pt_3 (trimer) show greater valance unsaturation than isolated Pt adatoms.

Description	Charge
Pt adatom	−0.16
Pt substituting for O	−0.15
Pt substituting for Al	+0.41
Pt#1 in trimer replacing O1	−0.29
Pt#2 in trimer replacing O2	−0.02
Pt#3 in trimer replacing Al	+0.19
Pt#1 in –OH capped Pt trimer	+0.73
Pt#2 in –OH capped Pt trimer	+0.42
Pt#3 in –OH capped Pt trimer	+0.85

Charge density analysis also gives insight into the origin of the anomalous Pt–Pt distances. Elongation of the Pt–Pt bonds when the Pt_3 structure is –OH capped results from a flow of electron from the Pt to the cap, thereby weakening the Pt–Pt bonds. This effect is visible in Figure 5, which shows electronic densities in the Pt_3 plane with and without the capping –OH group. The intensity scale is thermal, with red indicating the greatest electron density. Note the significant depletion of electron density between Pt atoms when the structure is –OH capped. This observation is further supported by Mulliken population analysis. The overlap populations for the three Pt–Pt bonds are (0.21, 0.02, −0.13) and (0.32, 0.41, −0.02) in the Pt_3OH and Pt_3 cases respectively. Again we see a clear indication of depletion of electron density from the Pt–Pt bonds when the structure is –OH capped.

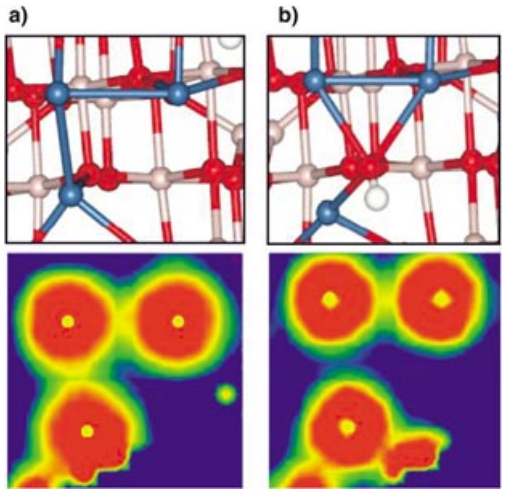

Figure 5. Upper images: Top-down view of Pt_3/γ-alumina (a) and Pt_3OH/γ-alumina (b). Lower images: Electronic density (thermal scale, red = high) in the Pt_3 plane corresponding to the image immediately above. Note the depletion of electron density in the Pt–Pt bonds when the structure is –OH capped.

Conclusions

In summary, subangstrom-resolution *Z*-STEM has revealed interesting Pt_3 clusters on the γ-alumina (110) surface. Theoretical calculations indicate that these structures are –OH capped Pt adatom trimers on the oxygen-terminated form of the (110C) surface. The anomalous Pt–Pt distances arise from depletion of electron density from the Pt–Pt bonds by the –OH capping structure.

Acknowledgements

This research was sponsored by the USDoE under Contract DE-FC02-01CH11085, by NSF-GOALI grant DMR-0111841 with Alcoa Inc., by the William A. and Nancy F. McMinn Endowment at Vanderbilt University, and by a DuPont Young Professor award to K.S.

 © 2004 Wiley-VCH Verlag GmbH & Co. KGaA, Weinheim

Computations were partially supported by NCSA-CHE990015N. We are grateful to R. D. Adams and M. Amiridis (University of South Carolina) for providing the catalyst sample.

Keywords: aluminum · density functional calculations · heterogeneous catalysis · platinum · scanning transmission electron microscopy (STEM)

[1] B. C. Gates, *Chem. Rev.* **1995**, *95*, 511.
[2] M. Che, C. O. Bennett, *Adv. Catal.* **1989**, *36*, 55.
[3] R. Shah, M. C. Payne, M.-H. Lee, J. D. Gale, *Science* **1996**, *271*, 1395.
[4] Z. Xu, F.-S. Xiao, S. K. Purnell, O. Alexeev, S. Kawi, S. E. Deutsch, B. C. Gates, *Nature* **1994**, *372*, 346.
[5] S. De Rossi, G. Ferraris, S. Fremiotti, E. Garrone, G. Ghiotti, M. C. Campa, V. Indovina, *J. Catal.* **1994**, *148*, 36; B. M. Weckhuysen, R. A. Schoonheydt, Catal. Today **51**, 223 (1999); R. L. Puurunen, B. G. Beheydt, B. M. Weckhuysen, *J. Catal.* **2001**, *204*, 253.
[6] S. J. Pennycook, A. Howie, M. D. Shannon, R. Whyman, *J. Mol. Catal.* **1983**, *20*, 345; P. L. Gai, K. Kourtakis, *Science* **1995**, *267*, 661; M. Valden, X. Lai, D. W. Goodman, *Science* **1998**, *281*, 1647; T. W. Hansen, J. B. Wagner, P. L. Hansen, S. Dahl, H. Topsoe, C. J. H. Jacobsen, *Science* **2001**, *294*, 1508.
[7] S. Helveg, J. V. Lauritsen, E. Lægsgaard, I. Stensgaard, J. K. Nørskov, B. S. Clausen, H. Topsøe, F. Besenbacher, *Phys. Rev. Lett.* **2000**, *5*, 951.
[8] P. D. Nellist, S. J. Pennycook, *Science* **1996**, *274*, 413.
[9] V. A. Nasluzov, V. V. Rivanenkov, A. M. Shor, K. M. Neyman, N. Rösch, *Chem. Phys. Lett.* **2003**, *374*, 487.
[10] J. R. Chang, S. L. Chang, T. B. Lin, *J. Catal.* **1997**, *169*, 338.
[11] M. Klimenkov, S. Nepijko, H. Kuhlenbeck, M. Bäumer, R. Schlögl, H.-J. Freund, *Surf. Sci.* **1997**, *391*, 27.
[12] M. Klimenkov, H. Kuhlenbeck, S. A. Nepijko, *Surf. Sci.* **2003**, *539*, 31.
[13] S. N. Rashkeev, K. Sohlberg, M. V. Glazoff, J. Novak, S. J. Pennycook, S. T. Pantelides, *Phys. Rev. B* **2003**, *67*, 115414.
[14] J. R. B. Gomes, Z. Lodziana, F. Illas, *J. Phys. Chem. B* **2003**, *107*, 6411.
[15] O. L. Krivanek, N. Dellby, A. R. Lupini, *Ultramicroscopy* **1999**, *78*, 1.
[16] W. Kohn, L. J. Sham, *Phys. Rev.* **1965**, *140A*, 1133.
[17] J. P. Perdew, *Phys. Rev. B* **1986**, *33*, 8822.
[18] A. D. Becke, *Phys. Rev. A* **1988**, *38*, 3098.
[19] M. C. Payne, M. P. Teter, D. C. Allan, T. A. Arias, J. D. Joannopoulos, *Rev. Mod. Phys.* **1992**, *64*, 1045,.
[20] K. Laasonen, R. Car, C. Lee, D. Vanderbilt, *Phys. Rev. B* **1991**, *43* , 6796; K. Laasonen, A. Pasquarello, C. Lee, R. Car, D. Vanderbilt, *Phys. Rev. B* **1993**, *47*, 10142.
[21] Monkhorst, H. J. , J. D. Pack, *Phys. Rev. B* **1976**, *13*, 5188.
[22] M. D. Segall, C. J. Pickard, R. Shah, M. C. Payne, *Mol. Phys.* **1996**, *89*, 571; M. D. Segall, R. Shah, C. J. Pickard, M. C. Payne, *Phys. Rev. B* **1996**, *54*, 16317.
[23] K. Sohlberg, S. J. Pennycook, S. T. Pantelides, *J. Am. Chem. Soc.* **1999**, *121*, 7493.
[24] J. H. de Boer, G. M. M. Houben, *Proc. Int. Symp. React. Solids* **1952**, *I*, 237.
[25] All-electron calculation performed here with: P. Blaha, K. Schwarz, J. Luitz, *WIEN97, A Full Potential Linearized Augmented Plane Wave Package for Calculating Crystal Properties*, (Karlheinz Schwarz, Techn. Univ. Wien, Vienna **1999**); Updated version of P. Blaha, K. Schwarz, P. Sorantin, S. B. Trickey, *Comp. Phys. Commun.* 1990, **59**, 399.
[26] H. Knözinger, P. Ratnasamy, *Catal. Rev. Sci. Eng.* **1978**, *17*, 31.
[27] K. Sohlberg, S. T. Pantelides, S. J. Pennycook, *Surf. Sci. Lett.* **2000**, *470*, L88.
[28] K. Sohlberg, S. J. Pennycook, S. T. Pantelides, *J. Am. Chem. Soc.* **1999**, *121*, 10999.
[29] K. Sohlberg, S. J. Pennycook, S. T. Pantelides, *Chem. Eng. Commun.* **2000**, *181*, 107.
[30] S. Wang, A. Y. Borisevich, S. N. Rashkeev, M. V. Glazoff, K. Sohlberg, S. J. Pennycook, S. T. Pantelides, *Nat. Mater.* **2004**, *3*, 143 .
[31] O. S. Alexeev, G. W. Graham, M. Shelef, R. D. Adams, B. C. Gates, *J. Phys. Chem. B* **2002**, *106*, 4697.
[32] K. Sohlberg, S. J. Pennycook, S. T. Pantelides in *Vol.* 4: *Recent Research Developments in Physical Chemistry, part 1*, **2000**, *71*.
[33] D. R. Jennison, A. Bogicevic, *Faraday Discuss.* **1999**, *114*, 45.
[34] K. Sohlberg, S. T. Pantelides, S. J. Pennycook, *J. Am. Chem. Soc.* **2001**, *123*, 26; L. J. Alvarez, J. F. Sanz, M. J. Capitán, M. A. Centeno, J. A. Odrlozola, *J. Chem. Soc. Faraday Trans.* **1993**, *89*, 3623.
[35] C. Wolverton, K. C. Hass, *Phys. Rev. B* **2001**, *63*, 024102.
[36] Hannu Karhu, Dissertation, University of Turku, **2003**. Key sections are available for download at http://www.physics.utu.fi/matsci/Karhu/index e.html.
[37] N. N. Greenwood, A. Earnshaw, *Chemistry of the Elements*, Pergamon Press, Oxford, **1984**, chapter 18.
[38] P. D. Nellist, private communication.

Received: May 6, 2004
Revised: September 11, 2004

Early View Article
Published online on November 17, 2004

 © 2004 Wiley-VCH Verlag GmbH & Co. KGaA, Weinheim